MIMO CHANNEL SOUNDING TAKING INTO ACCOUNT SMALL ANGULAR SPREAD

Tobias P. Kurpjuhn
kurpjuhn@nws.ei.tum.de

Wolfgang Utschick
utschick@nws.ei.tum.de

Institute for Circuit Theory and Signal Processing
Technische Universität München, Munich, Germany

ABSTRACT

In the last years the use of multiple receive antennas as well as multiple transmit antennas has attracted worldwide attention to extend existing mobile communication systems with respect to their performance. Therefore it is of great importance to know the features of the real propagation channel. To this end, the real propagation channel is investigated by MIMO Channel Sounding, where high-resolution parameter estimation schemes are used to resolve the physical channel with respect to their spatial (and temporal) structure. However, due to narrow diffuse scatterers the commonly used model of discrete wavefronts is no longer valid.

In this article we introduce a simple approach to model wavefronts with small angular spread. Additionally, we show that the ESPRIT algorithm with a slight modification is applicable to jointly estimate the direction of arrival and the angular spread. The approach is based on the assumption of Gaussian distributed wavefronts.

1. INTRODUCTION

One of the most innovative and fastest growing sectors of industry is the mobile communication market, which experiences a big push to extend existing systems with respect to an increased performance, not only because of the growing number of subscribers, but also due to the increasing demands regarding *quality of service* (QoS) and data rate. Thereby the use of multiple receive antennas as well as multiple transmit antennas has attracted worldwide attention in the last years. Such systems are denoted as *multiple-input-multiple-output* (MIMO) systems. The proposals to exploit the potentialities of MIMO systems are very variegated (e.g. BLAST [1] and Eigenbeamforming [2] in various versions). However, just as various as the system proposals are the requests for the channel. Therefore, it is of fundamental interest to have detailed knowledge of the properties of the real MIMO propagation channel between transmitter and receiver to rank and differentiate the different system proposals with respect to their performance under real conditions. To this end, high-resolution parameter estimation schemes, such as SAGE [3], MUSIC [4], ESPRIT [5, 6] and many more, have obtained new interest to measure the real MIMO propagation channel by means of a geometric interpretation [7]: *MIMO Channel sounding*.

The high-resolution parameter estimation schemes are used to resolve the measured channel transfer function into single wavefronts, which are usually characterized by the *direction of arrival* (DOA), propagation delay, Doppler frequency and power. The most commonly used model for a wavefront in the wireless channel has been a point source model which corresponds to discrete DOAs [8]. However, due to the presence of scatterers in a real environment the spatial signature of each wavefront can no longer be parameterized by a discrete direction of arrival alone. The presence of narrow diffuse scattering occurring in real radio channel measurements will cause small angular spread [9]. The assumption of mere discrete rays becomes restrictive and would lead to estimation errors.

One method to compensate for this effect is to increase the number of discrete wavefronts that have to be estimated. Thereby the spread wavefront will hopefully be approximated be several discrete wavefronts.

A more promising method is to adopt the signal model and to assume wavefronts with angular spread according to a suitable distribution function. As a consequence the impinging wavefronts are now parameterized by their nominal direction θ and a parameter σ of the distribution function. Recently some methods have been proposed to estimate the DOAs and the angular spread, based on multidimensional search [10]. Other methods have been proposed to estimate the spatial signature [11, 12] of the impinging wavefronts.

In this work we introduce a simple model for wavefronts with Gaussian distributed angular spread. The angular spread is assumed small so that the the angular spread has not yet led to a numerical increase in the rank. Additionally we provide a method to jointly estimate the DOA and the angular spread with a modified ESPRIT algorithm.

2. DATA MODEL

2.1. Point Source Model

Assuming a single source with multipath propagation, impinging with L rays at a uniform linear array (ULA) with M antennas under the influence of additive white Gaussian

noise produces the data model

$$\boldsymbol{x}(t) = \sum_{n=1}^{L} \rho_n \boldsymbol{a}(\theta_n) \cdot s(t) + \boldsymbol{n}(t), \tag{1}$$

where ρ_n denotes the complex amplitude of each wavefront, $\boldsymbol{a}(\theta_n)$ denotes the steering vector of one wavefront, $s(t)$ denotes the transmitted signal, and $\boldsymbol{n}(t)$ denotes the complex, white Gaussian noise.
Under the assumption of discrete wavefronts, the steering vectors $\boldsymbol{a}(\theta_n)$ are parameterized only by the nominal DOA θ_n. The steering vector can be written as

$$\boldsymbol{a}_n = \left[1; e^{\mathrm{j}\mu_n}; \cdots; e^{\mathrm{j}(M-1)\mu_n}\right]^{\mathrm{T}}, \tag{2}$$

where $()^{\mathrm{T}}$ denotes the transpose of a vector and

$$\mu_n = -2\pi\Delta \sin(\theta_n) \tag{3}$$

is the spatial frequency with antenna spacing Δ in fractions of the wavelength.

2.2. Distributed Source Model

Giving up the point source model and going to a more realistic channel model, where each propagation path consists of a large number of sub-paths being distributed around the nominal direction θ_n, leads to the distributed source model. To this end, a steering vector with small angular spread can be modeled as

$$\boldsymbol{w}(\theta_n) = \rho_n \cdot \sum_k \boldsymbol{a}(\theta_n + \vartheta_k), \tag{4}$$

where $\boldsymbol{w}(\theta_n)$ denotes the spread steering vector which consists of a sum over a huge, possibly infinite, number of discrete sub-paths $\boldsymbol{a}(\theta_n + \vartheta_k)$. This wave-packet is centered around a nominal direction θ_n and ϑ_k is distributed according to a given distribution. The whole wave-packet is given a complex amplitude ρ_n. Note, that the model in Eq. (4) is only valid for small angular spread.
In the sequel we will work with the normalized version of the spread steering vector

$$\boldsymbol{v}(\theta_n) = \frac{1}{\rho_n} \cdot \boldsymbol{w}(\theta_n) = \sum_k \boldsymbol{a}(\theta_n + \vartheta_k). \tag{5}$$

In the following we are assuming that the sub-paths $\boldsymbol{a}(\theta_n + \vartheta_k)$ are Gaussian distributed around the nominal DOA θ_n with standard deviation σ_n. This seems a reasonable assumption, since the biggest portion of the sub-paths are concentrated around the main direction and large deviations from the nominal direction are less likely [13]. Additionally it seems reasonable to assume a symmetric distribution. The proximate distribution function is the Gaussian distribution. According to [13] the distribution function is not critical, as long as the angular spread is small.
For simplicity we are assuming an infinite number of sub-paths. Additionally we assume the Gaussian function to be zero outside of $\theta_n \pm 4\sigma_n$. With these assumptions the spread steering vector can be written as

$$\begin{aligned} \boldsymbol{v}(\theta_n, \sigma_n) &= \sum_{k=1}^{\infty} \boldsymbol{a}(\theta_n + \vartheta_k) \\ &= \int_{\theta_n - 4\sigma_n}^{\theta_n + 4\sigma_n} \boldsymbol{a}(\vartheta) \cdot \mathcal{N}(\theta_n, \sigma_n^2)\, \mathrm{d}\vartheta, \end{aligned} \tag{6}$$

where $\mathcal{N}(\theta_n, \sigma_n^2)$ denotes the normal distribution function with mean θ_n and variance σ_n^2. The m-th entry of the steering vector $\boldsymbol{v}(\theta_n, \sigma_n)$ for a wavefront with small Gaussian distributed angular spread $v_m(\theta_n, \sigma_n)$ reads as

$$\begin{aligned} &v_m(\theta_n, \sigma_n) = \\ &= \int_{\theta_n - 4\sigma_n}^{\theta_n + 4\sigma_n} \frac{\exp\left(-\frac{(\vartheta - \theta_n)^2}{2\sigma_n^2} - \mathrm{j}(m-1)2\pi\Delta \sin(\vartheta)\right)}{\sqrt{2\pi}\sigma_n}\, \mathrm{d}\vartheta. \end{aligned} \tag{7}$$

Unfortunately the integration in Eq. (7) cannot be solved analytically.

3. EFFECT OF ANGULAR SPREAD

Eq. (7) computes the steering vector of a wavefront, normal distributed around the main direction θ_n with a standard deviation σ_n. To get a better insight into the effects of angular spread to judge the demand for an estimation scheme, we numerically evaluate the ratio $r(m) = |v_m|/|v_1|$. Figure 1 shows this ratio for $m \in \{1, \cdots, 10\}$ for a wavefront, impinging from direction $\theta = 30°$ for different standard deviations of the Gaussian distribution.

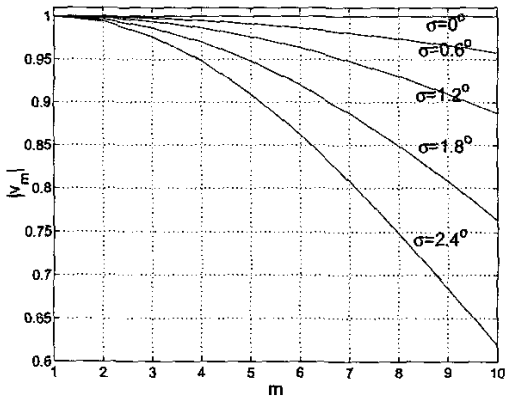

Fig. 1. Ratio $r(m) = |v_m|/|v_1|$ of a spread steering vector from $\theta = 30°$ for different standard deviations $\sigma = \{0°, 0.6°, 1.2°, 1.8°, 2.4°\}$.

It can be seen, that the correlation decreases with increasing

angular spread σ and increasing element number m. This influence indicates the effect of angular spread to reduce the mutual correlations between the antenna elements, which has been described previously [14].

When comparing the steering vector with angular spread and the steering vector without angular spread with regard to the complex phase it can be seen that the complex phase is influenced only by a rather tiny amount.

4. APPROXIMATION OF ANGULAR SPREAD

Proper DOA and angular spread estimation requires extracting the parameters of the function $\boldsymbol{v} = \boldsymbol{f}(\theta, \sigma)$. To this end, the analytic solution of Eq. (7) is required. Unfortunately the integral cannot be solved analytically and therefore an analytical inversion is also not possible. To circumvent this problem, we introduce two approximations for the integration:

First, we approximate the Gaussian distribution by a polynomial of second order and secondly, we model the steering vector $\boldsymbol{a}(\theta_n + \vartheta)$ by a Taylor series of second order at the operating point θ_n.

The approximation of the Gaussian distribution can be written as

$$\begin{aligned} \mathcal{N}(\theta_n, \sigma_n^2) &= \frac{1}{\sqrt{2\pi}\sigma_n} e^{-\frac{(\vartheta-\theta_n)^2}{2\sigma_n^2}} \\ &\approx \alpha_1(\vartheta-\theta_n)^2 + \alpha_2(\vartheta-\theta_n) + \alpha_3. \end{aligned} \tag{8}$$

Constructing the polynomial such that the maximum value of the polynomial and the maximum value of the Gaussian distribution coincide and that the polynomial has unity surface between the two intersections with the abscissa, yields

$$\alpha_1 = -\frac{16}{9(\sqrt{2\pi}\sigma_n)^3}\ ;\ \alpha_2 = 0\ ;\ \alpha_3 = \frac{1}{\sqrt{2\pi}\sigma_n}. \tag{9}$$

Figure 2 compares this approximation with the original Gaussian function.

In our second approximation, we model the steering vector $\boldsymbol{a}(\theta_n+\vartheta)$ by a Taylor series of second order at the operating point θ_n. The solution reads

$$\boldsymbol{a}(\theta_n+\vartheta) \approx \boldsymbol{a}(\theta_n) + \boldsymbol{a}'(\theta_n)(\theta_n-\vartheta) + \boldsymbol{a}''(\theta_n)\frac{(\theta_n-\vartheta)^2}{2}, \tag{10}$$

where the derivations are performed with respect to θ_n. With these two approximations the integration from Eq. (7) can now be solved. Performing the integration between the two intersections with the abscissa of the polynomial from Eq. (8) yields the solution

$$\boldsymbol{v}_{approx}(\theta_n, \sigma_n) = \boldsymbol{a}(\theta_n) + \frac{11\cdot\pi\cdot\sigma_n^2}{80}\cdot\boldsymbol{a}''(\theta_n). \tag{11}$$

Note, that the solution contains no first-order derivative. This matches with the assumption of a symmetric distribution of the sub-paths.

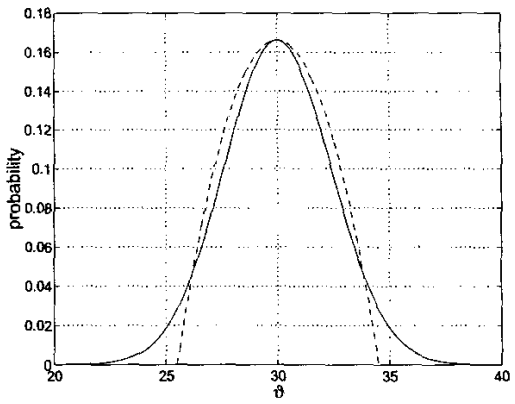

Fig. 2. The Gaussian function (solid line) and its approximation by a polynomial of second order (dashed line). The used Gaussian function represents the density of one path impinging from $\theta_n = 30^o$ with standard deviation of $\sigma_n = 2.4^o$.

Figure 3 compares the approximation $\boldsymbol{v}_{\text{approx}}(\theta_n, \sigma_n)$ from Eq. (11) with the numerical derived steering vector $\boldsymbol{v}(\theta_n, \sigma_n)$ from Eq. (7). It can be seen that the approximated model

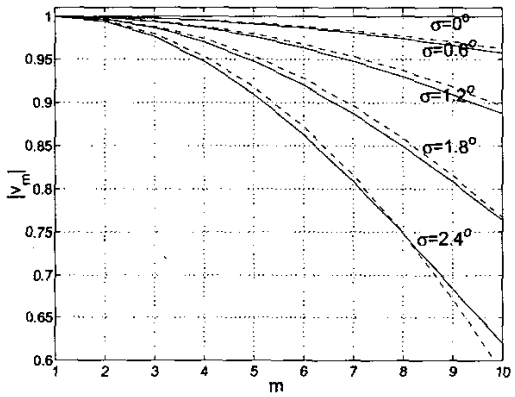

Fig. 3. Ratio $r(m) = |v_m|/|v_1|$ of a spread steering vector from $\theta = 30^o$ for different standard deviations $\sigma = \{0^o, 0.6^o, 1.2^o, 1.8^o, 2.4^o\}$ (solid line), compared with the approximation (dashed lines).

matches very well with the numerical solution

5. DOA AND ANGULAR SPREAD ESTIMATION

The simple analytical formula for a steering vector, produced by a small Gaussian distributed wavefront in Eq. (11), gives raise to a new concept for estimating the DOA and the standard deviation of the distribution function. One approach would be for example to replace the array response vector of Eq. (2) by Eq. (11) for the optimization of the ML

function. Thereby, not only the parameter set $\{\theta_n\}$ has to be chosen, but also the corresponding set $\{\sigma_n\}$. The procedure is very straightforward.
Here we want to show, that also a linear estimation technique, in particular ESPRIT, can be extended to be applicable to this estimation task.

5.1. Estimation with ESPRIT

The ESPRIT algorithm performs the DOA estimation by exploiting the shift-invariance property of two overlapping subarrays of a ULA [5, 6]. Due to this shift-invariance property the antenna signals of two overlapping subarrays differ only by a complex factor, which is directly related to the DOA.
The equation for the shift-invariance property reads as

$$\boldsymbol{J}_1 \cdot \boldsymbol{A} \cdot \operatorname{diag}\{\psi_n\}_{n=1}^{d} = \boldsymbol{J}_2 \cdot \boldsymbol{A}, \tag{12}$$

where $\boldsymbol{J}_1$ and $\boldsymbol{J}_2$ denote selection matrices cutting out only the first $(M-1)$ and the last $(M-1)$ lines of the subsequent matrix, respectively. The matrix $\boldsymbol{A} = [\boldsymbol{a}_1 \ldots \boldsymbol{a}_d]$ comprises the steering vectors of the d wavefronts. It is well known [6], that the equation

$$\boldsymbol{A} = \boldsymbol{U}_s \cdot \boldsymbol{T}, \tag{13}$$

holds, where $\boldsymbol{U}_s$ are the d dominant eigenvectors of the covariance matrix of the received signal (denoted as signal subspace) and $\boldsymbol{T} \in \mathbb{C}^{d \times d}$ is a matrix of full rank.
Inserting this in Eq. (12), we obtain the values ψ_n as the eigenvalues of

$$\boldsymbol{\Phi} = (\boldsymbol{J}_1 \cdot \boldsymbol{U}_s)^{+} \cdot (\boldsymbol{J}_2 \cdot \boldsymbol{U}_s), \tag{14}$$

where $()^{+}$ denotes the pseudo-inverse.

5.1.1. Discrete wavefronts

In the case of discrete wavefronts the complex coefficients ψ_n are only a function of the DOA. In particular,

$$\psi_n = \exp(\mathrm{j}\mu_n), \tag{15}$$

where μ_n is the spatial frequency, c.f. Eq. (3).

5.1.2. Angular Spread

In the case of spread wavefronts the complex factor is a function of the DOA and the standard deviation of the Gaussian distribution function of the angle. After having solved the invariance equation of Eq. (14) to obtain the complex factors ψ_n we have to map back the complex factors to the parameters θ_n and σ_n. Note, that the invariance equation was designed to operate on Vandermonde vectors, however, it is still able to deal with angular spread, if the results ψ_n are interpreted and processed differently. The functional connection is

$$\boldsymbol{J}_1 \cdot \boldsymbol{v}(\theta_n, \sigma_n) \cdot \psi_n = \boldsymbol{J}_2 \cdot \boldsymbol{v}(\theta_n, \sigma_n), \tag{16}$$

according to Eq. (11) and (12).

5.2. Simulations

Eq. (16) gives the analytical relationship between the complex factor provided by the invariance equation of ESPRIT and the parameters of the Gaussian distributed wavefront. Estimating the complex factor ψ_n provides a direct estimate for the DOA and the standard deviation of the distributed wavefront. To find the right parameter set θ_n and σ_n, we use an gradient based optimization algorithm. First, we choose a test parameter set $\hat{\theta}$ and $\hat{\sigma}$ and compute the corresponding $\psi(\hat{\theta}, \hat{\sigma})$. Then we modify $\hat{\theta}$ and $\hat{\sigma}$ by a small increment to approach ψ_n from the invariance equation. To this end, we minimize

$$\min_{\theta,\sigma} |\psi_n - \psi(\theta, \sigma)|^2, \tag{17}$$

where we minimize the squared absolute value since ψ_n is approximately Gaussian distributed for Gaussian distributed noise. For each wavefront a 2D minimization has to be performed. Figure 4 shows a typical shape of the cost function of Eq. (17). It can be seen, that only one distinct minimum

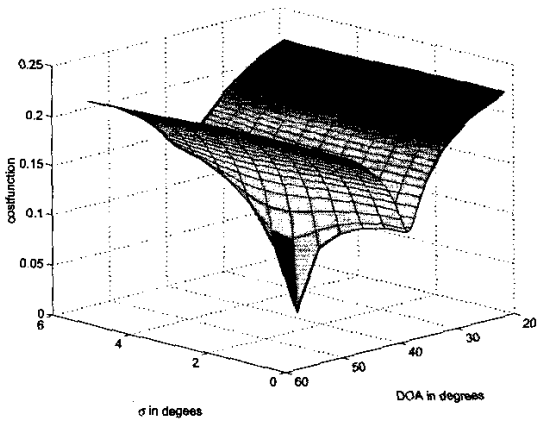

Fig. 4. Shape of the cost function at high SNR ($\theta = 38.5°, \sigma = 3°$).

exists. The standard approach to retrieve the nominal DOA from ψ_n (c.f. Eq. (15)) provides a first and close starting point for this optimization. Therefore, the minimization is well-behaved and can be accomplished in very few steps.

Figure 5 shows the RMSE as a function of the SNR for a scenario with two wavefront with the parameters $\{\theta_1, \sigma_1\} = \{38.5°, 3°\}$ and $\{\theta_2, \sigma_2\} = \{-25°, 0.1°\}$ at an 8-ULA with 1024 BPSK samples. We compute the RMSE for the DOAs

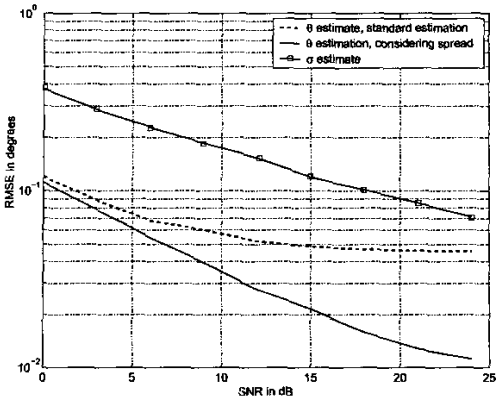

Fig. 5. RMSE in degrees of the estimated DOAs with standard estimation (dashed line) and considering the angular spread (solid line) for two impinging DOAs with different spread.

as

$$\mathrm{RMSE}_\theta = \sqrt{\frac{1}{N}\sum_{i=1}^{N} \|\hat{\boldsymbol{\theta}}_i - \boldsymbol{\theta}\|_2^2}, \qquad (18)$$

where N, $\boldsymbol{\theta}$ and $\hat{\boldsymbol{\theta}}_i$ denote the number of trials, the vector of the real DOAs and the vector of the estimated DOAs, respectively. The same applies for the standard deviation

$$\mathrm{RMSE}_\sigma = \sqrt{\frac{1}{N}\sum_{i=1}^{N} \|\hat{\boldsymbol{\sigma}}_i - \boldsymbol{\sigma}\|_2^2}. \qquad (19)$$

It can be seen, that for increasing SNR the standard estimation approach starts to saturate, while for the modified ESPRIT the RMSE of the estimated DOAs continuous to decrease. However, note that the RMSE of the modified ESPRIT also starts to saturate at high SNR which is due to the fact, that the modified ESPRIT works with an approximation, c.f. Eq. (11), of the continuously spread wavefront, c.f. Eq. (6).

6. CONCLUSION

In this article we have presented a closed form expression of a steering vector, modeling a wavefront with small, Gaussian distributed angular spread. In the end we have extended the ESPRIT algorithm for jointly estimating the DOA and the standard deviation of the wavefront. The simulation showed that the new, extended estimation approach avoids a saturation of the RMSE of the DOA due to an angular spread for increasing SNR. Additionally the standard deviation of the distribution function of the angle can be estimated. This approach seems suitable for channel sounding in real channel situations, where the model of discrete wavefronts is not valid.

7. REFERENCES

[1] Foschini G. J., "Layered space-time architectures for wireless communications in a fading environment," in *Bell Labs Technical Journal*, 1996, pp. 41–59.

[2] Brunner C., Utschick W., and Nossek J.A., "Exploiting the short-term and long-term channel properties in space and time: Eigenbeamforming concepts for the BS in WCDMA," in *European Transactions on Telecommunication*, 2001, vol. 12, No. 5, pp. 365–378.

[3] M. Feder and E. Weinstein, "Parameter estimation of superimposed signals using the EM algorithm," *IEEE Trans. Acoustics, Speech, and Signal Processing*, vol. 36, pp. 477–489, Apr. 1988.

[4] R. O. Schmidt, "Multiple emitter location and signal parameter estimation," in *Proc. RADC Spectrum Estimation Workshop*, Griffiths AFB, NY, 1979, pp. 243–258, reprinted in *IEEE Trans. Antennas and Propagation*, vol. 34, pp. 276–280, March 1986.

[5] R. Roy and T. Kailath, "ESPRIT - estimation of signal parameters via rotational invariance techniques," *IEEE Trans. Acoustics, Speech, and Signal Processing*, pp. 984–995, July 1989.

[6] A. Paulraj, R. Roy, and T. Kailath, "Estimation of signal parameters via rotational invariance techniques - ESPRIT," in *Proc. 19th Asilomar Conf. on Signals, Systems, and Computers*, Pacific Grove, CA, Nov. 1985, pp. 83–89.

[7] M. Toeltsch, J. Laurila, K. Kalliola, A. F. Molisch, and E. Bonek, "Statistical characterization of urban spatial radio channels," in *IEEE Journal on Selected Areas in Communications*, Dec. 2001.

[8] J. J. Blanz and P. Jung, "A flexibly configurable spatial model for mobile radio systems," *IEEE Trans. Communications*, vol. 46, pp. 367–371, Mar. 1998.

[9] B. Fleury, P. Jourdan, and A. Stucki, "High-resolution channel parameter estimation for MIMO applications using the SAGE algorithm," in *Proc. International Zurich Seminar on Broadband Communication*, Zurich, Switzerland, Feb. 2002.

[10] T. Trump and B. Ottersten, "Estimation of nominal direction of arrival and angular spread using an array of sensors," *Proceeding of COST 229 Adaptive Systems, Intelligent Approaches, Massively Parallel Computing and Emergent Techniques in Signal Processing and Communications*, Jan. 1995.

[11] D. Asztely and B. Ottersten, "The effects of local scattering on direction of arrival estimation with music and esprit," *Proc. IEEE Int. Conf. Acoust., Speech, Signal Processing*, Feb. 1998.

[12] D. Asztely, B. Ottersten, and A. Swindlehurst, "A generalized array manifold model for local scattering in wireless communications," *Proc. IEEE Int. Conf. Acoust., Speech, Signal Processing*, Jan. 1997.

[13] T. Trump and B. Ottersten, "Estimation of nominal direction of arrival and angular spread using an array of sensors," *Signal Processing*, vol. 50, pp. 57–69, Apr. 1996.

[14] J. Salz and J. Winters, "Effect of fading correlation on adaptive arrays in digital mobile radio," *IEEE Trans. Vehicular Technology*, vol. 43-4, pp. 1049–1057, Nov. 1994.